ARCHIVES OF ACOUSTICS
10, 3, 281–302 (1985)

FLOW PERTURBATION MEASUREMENTS BY NUMERICAL ANALYSIS OF THE POWER SPECTRUM OF A DOPPLER SIGNAL

MACIEJ PIECHOCKI

Institute of Fundamental Technological Research, Polish Academy of Sciences
(00–049 Warsaw, ul. Świętokrzyska 21)

A method was elaborated to measure flow perturbations. It was based on analysis of the power spectrum of a Doppler signal. In view of the simplifications assumed, it concerns pulsed flowmetres. The process of the formation of the Doppler signal is described mathematically, its power spectrum is calculated. A numerical model of the signal power spectrum is pressented. It has been constructed to calculate the effect of the gradient of the mean velocity in the sample volume, and also to determine the effect of the passage of blood particles through the sample volume on the shape of the power spectrum.

This model was verified experimentally. On the basis of it, a corrected turbulence index was proposed. This index describes with greater precision the flow perturbations.

1. Introduction

The introduction of measurements of the degree of the perturbation into diagnostic studies of the circulatory system results from a tendency to expand the application range of Doppler flowmeters, by fuller use of information on the flow contained in the signal obtained. The measurement of perturbations permits the quantization of the flow properties, which are now evaluated qualitatively from the detection of Doppler signals. The published investigations confirm the usefulness of such a measurement in studies on the stenosis of blood vessels and on the intra-operational investigations of the correctness of the vessel reconstruction [5, 8].

The commonly applied measure of the flow perturbation is the so-called turbulence index, defined as the percentage ratio between the standard deviation and the mean frequency of the power spectrum of a Doppler signal or its time interval histogram [5, 8].

In considerable approximation, it is assumed that if the velocity measurement is carried out with a sample volume that is small compared with the size of a vessel, the indices mentioned above correspond approximately to the ratio between the standard deviation of the instantaneous velocity oscillation and the mean velocity in the area studied. For laminar flow, the value of the turbulence index should, therefore, be zero [8]. Unfortunately, the interpretation given here is only too oversimplified. For, in practice, the values of the turbulence index never drop down to zero, as the width of the power spectrum also depends on factors other than flow perturbation. Because of this, the indices presented here are hardly sensitive to the real magnitude of flow perturbations.

Another essential problem, occurring for flow perturbation measurements, which, however, will be reflected here, is the difficulty in obtaining accurate estimation of a Doppler signal power spectrum for real, pulsating blood flows. This involves difficulties in accurate measurement of the turbulence index.

The aim of this paper is to analyze relations between the flow studied and the power spectrum of a Doppler signal and to develop a method permitting a more precise flow perturbation measurement than that allowed by the turbulence index. It was assumed that the shape of the sample volume and the distribution of the mean velocity inside this volume can be just any.

The process of the generation of the Doppler signal was described and its power spectrum calculated in order to determine factors defining the parameters of this spectrum. The dependencies obtained permitted the construction of an approximate, numerical method for the calculation of the power spectrum and its parameters, based on measurements of the mean flow velocity profile in a vessel and the parameters of the flowmeter. By comparing the power spectrum, measured for a given signal and a synthesized one, we can conclude on the existence of flow perturbations.

A numerical model of the power spectrum of a signal is also the basis for the introduction of an improved turbulence index, proposed in this paper. This index is defined in a way that is slightly different than that given in the literature. From the spectrum variance the effects are detracted which are related to the factors expanding the spectrum, and not connected with the flow perturbations. The detracted values can be determined numerically from measurements of the shapes of the samples volumes and the mean profiles of the flow velocity.

2. Signal generation process

The description of the signal generation process aims at obtaining a mathematical form of a Doppler signal, depending on the properties of the investigated flow and on the parameters of the equipment. This description provides the

basis for calculating the signal power. To that end, analysis was successively performed on operations implemented by a typical Doppler flowmeter (Fig. 1) and on the effect of these operations on the final form of the signal.

The following assumptions were made:

1. The signal detected by the transducer is the sum of independent dissipations from randomly placed particles.

2. The amplitudes and phases of scattered waves are random.

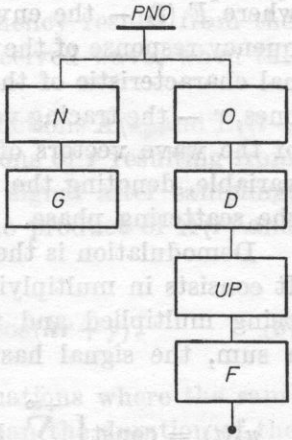

Fig. 1. A simplified schematic diagram of a flowmeter with pulsed emission. *G* — generator, *N* — transmitter, *O* — receiver, *D* — demodulator, *UP* — sampling unit, *F* — low-pass filter, *PNO* — transmit-receive transducer

3. All the scatterred waves, giving significant components of a signal with respect to the noise field, come from the nearest sample volume.

4. The sample volume is so small and far from the transducer that the scattered waves reaching the transducer can be recognized as plane.

5. The velocity of the scattering particles is constant in the course of passing through the sample volume and is parallel to the flow axis.

The first two assumptions are generally assumed in the analysis of a Doppler signal [16, 24] and lead to a random model of this signal.

A third assumption aims at avoiding the components of the signal which do not come from the sample volume and which can occur as a result of the known phenomenon of ambiguity in the measurement of distance by the impulsed apparatus [10].

The fifth assumption is satisfied for laminar flow in straight vessels. For perturbed flows, it is reduced to the requirement that the sample volume should be respectively small.

For a pulsed flowmeter, the voltage exciting the transmitter transducer to vibrate has the form:

$$x(t) = \sum_{n=-\infty}^{+\infty} E(t-n\tau_p)\cos\omega_0(t-n\tau_p), \qquad (1)$$

where $E(t)$ — the envelope of the transmitted impulse, ω_0 — the working frequency of the flowmeter, τ_p — the repetition period of the transmitted impulse. Thus, the signal $x(t)$ is an infinite sum of the identical pules.

With the given assumptions, the voltage at the receiving transducer, generated by the sum of waves scattered by a single particle, is expressed by

$$u_0(t) = \text{const}\Big[\sum_{n=-\infty}^{+\infty} E_1(t-n\tau_p-\boldsymbol{kr}/\omega_0)\Big]\, aA(\boldsymbol{r})\cos(\omega_0 t-\boldsymbol{kr}+\gamma), \tag{2}$$

where $E_1(t)$ — the envelope of the transmitted impulse, modified by the frequency response of the transducer at detection; $A(\boldsymbol{r})$ — the resultant directional characteristic of the transducer, made up of the transmitted and received ones, $\boldsymbol{r}$ — the tracing vector of the particle, describing its position, $\boldsymbol{k}$ — the sum of the wave vectors of the transmitted and scattered waves, a — a random variable, denoting the scattering amplitude, γ — a random variable denoting the scattering phase.

Demodulation is the first operation carried out on the received signal $u_0(t)$. It consists in multiplying the signal by a sinusoid at the frequency ω_0. After being multiplied and transforming the product of the cosine function into a sum, the signal has the form

$$u_d(t) = \text{const}\Big[\sum_{n=-\infty}^{+\infty} E_1(t-n\tau_p-\boldsymbol{kr}/\omega_0)\Big]\, aA(\boldsymbol{r})\times$$

$$\times 1/2\,[\cos(-\boldsymbol{kr}+\gamma)+\cos(2\omega_0 t-\boldsymbol{kr}+\gamma)]. \tag{3}$$

It is the sum of two components. The first, related to $\cos(\boldsymbol{k}, \boldsymbol{r}+\gamma)$, which changes slowly (through the dependence of $\boldsymbol{r}$ on time), is the one of interest. The other, related to the curve of a double carrier frequency $2\omega_0$, can easily be filtered off, without losing information on the particle velocity. Thus, the final result of the demodulation will have the form

$$u_d(t) = \text{const}\Big[\sum_{n=-\infty}^{+\infty} E_1(t-n\tau_p-\boldsymbol{kr}/\omega_0)\Big]\, aA(\boldsymbol{r})\cos(\boldsymbol{kr}-\gamma). \tag{4}$$

Sampling operation

Another operation which is performed on a signal in a pulsed flowmeter is signal sampling in order to define the depth at which its analysis is carried out. This sampling will be written as a multiplication of the signal $u_d(t)$ by the sampling function $f_p(t)$, which is a periodic function with the period τ_p. Let us now introduce a delay t_r of this function with respect to the transmitter, correspond-

ing to the depth analysed. The form of the signal is, after the operation of sampling, given by the following formula

$$u_p(t) = \text{const}\Big[\sum_{n=-\infty}^{+\infty} f_p(t-n\tau_p-t_r)E_1(t)-n\tau_p-\boldsymbol{kr}/\omega_0)\Big]\times$$
$$\times aA(\boldsymbol{r})\cos(\boldsymbol{kr}+\gamma). \quad (5)$$

It is usually assumed that the sampling function is a sequence of Dirac impulses $\delta(t)$. The time difference between particular samples equals the repetition period of the transmitter impulses. The filling is a sinusoidal function with a frequency coresponding to the movement of a particle. This frequency results from the Doppler effect, i.e., a change in the frequency of the received wave, when the source or observer moves.

The envelope of the signal $u(t)$ is the product of the functions $A(\boldsymbol{r})$ and $E_1(t-$ $-n\tau_p-\boldsymbol{kr}/\omega_0)$ for $t = n\tau_p+t_r$ and the successive positions of $\boldsymbol{r}$ resulting from the movements of a particle. Thus, in describing the signal after sampling, we can introduce the function $H(\boldsymbol{r}, t_r)$, representing the product of $A(\boldsymbol{r})$ and $E_1(t-n\tau_p-\boldsymbol{kr}/\omega_0)$ for $t = n\tau_p-t_r$, namely:

$$u_p(t) = \text{const}\Big[\sum_{n=-\infty}^{+\infty}\delta(t-n\tau_p-t_r)\Big]\, aH(\boldsymbol{r}, t_r)\cos(\boldsymbol{kr}+\gamma). \quad (6)$$

However, in practice, we meet quite frequently situations where the sampling duration (when $f_r(t) \neq 0$) is equal to or greater than the duration of the transmitted impulse (when $E_1(t) \neq 0$). In practical solutions, as a rule systems calculating the mean value of a sample and memorizing it until the next value comes are used. Such a solution maximizes the energy contained in the spectrum concentrated around zero with respect to the remaining replications. By introducing the averaging process into our notation, we can simplify it. Thus, again, for a constant time delay we can define the function $H(\boldsymbol{r}, t_r)$ describing the envelope of the signal $u_p(t)$ defined by a change in the position of a particle [14].

$$H(\boldsymbol{r}, t_r) = \int_{-\infty}^{+\infty} f_p(\tau)E_1(\tau+t_r-\boldsymbol{kr}/\omega_0)\,d\tau A(\boldsymbol{r}). \quad (7)$$

Again, the signal after the sampling operation can be written in the form of a sequence of impulses set for $\tau = 0$,

$$u_p(t) = \text{const}\Big[\sum_{n=-\infty}^{+\infty}\delta(t-n\tau_p-t_r)\, aH(\boldsymbol{r}, t_r)\cos(\boldsymbol{kr}-\gamma). \quad (8)$$

The final form of the Doppler signal

The function $H(\boldsymbol{r}, t_r)$ describes the effective, from the viewpoint of the spectrum of the signal received, distribution of acoustic energy in space, which is usually called the sample volume. In further considerations, the parameter

t_r will be regarded as constant, i.e., the position of the sample volume in the flow field will be considered constant.

In order to obtain the total signal form after sampling it is necessary to sum up the contributions coming from all the particles. This procedure results from the independence of particular scatterings. The summary signal at the input of the sampling system will thus have the form

$$u_s(t) = \text{const}\Big[\sum_{n=-\infty}^{+\infty} \delta(t-n\tau_p-t_r)\Big]\Big[\sum_{i=1}^{N} a_i H(\boldsymbol{r}_i)\cos(\boldsymbol{k}\boldsymbol{r}+\gamma_i)\Big], \tag{9}$$

where N is the number of particles occurring at the same time in the sample volume.

The position of the particle $\boldsymbol{r}_i$ is a function of time. We assumed that the particle velocity $\boldsymbol{v}_i$ was constant and parallel to the flow axis as the particle flowed through the sample volume. The position of the particle can be given as

$$\boldsymbol{r}_i = \boldsymbol{r}_i^0 + \boldsymbol{v}_i t, \tag{10}$$

where $\boldsymbol{r}_i^0$ is the tracing vector of the particle for the time $t = 0$. The product of the position $\boldsymbol{r}$ and the wave vector $\boldsymbol{k}$ equals that of the Doppler frequency and time.

In addition, we can introduce the notation

$$a_i = \boldsymbol{k}\boldsymbol{r}_i^0. \tag{11}$$

a_i is a random variable with a distribution related to the distribution of the initial position of the particle in the sample volume, which from the assumption is taken as uniform.

Thus, the signal takes the following form:

$$u_s(t) = \text{const}\Big[\sum_{n=-\infty}^{+\infty} \delta(t-n\tau_p-t_r)\Big]\Big[\sum_{i=1}^{N} a_i H(\boldsymbol{r}_i)\cos(\omega_i t+a_i+\gamma_i)\Big]. \tag{12}$$

In this equation, the quantities a_i, a_i, γ_i, ω_i and $\boldsymbol{r}_i$ are random variables. The signal $u_s(t)$ (formula (12)) is the sum of functions of these quantities. Since the number of the factors summed up is very large (N is of the order of 10^6), and the probability distributions for each component of it are the same, $u_s(t)$ is a random, approximately Gaussian, process. For this process to be stationary, i.e., for the probabilistic quantities related to it to be constant in time, the flow field must be stationary. In addition, we assume that this is an ergodic process — where the values averaged over the set equal respectively the corresponding values averaged in time. In these conditions, all the information available on this process is contained in its second-order characteristics, i.e., in the auto-correlation function or the power spectrum.

Thus, to obtain maximum information on this flow, we should look for it in one of these measured characteristics. Such a solution would require, however, an extremely complicated measurement equipment and a good theoretical description of the process of spectrum formation.

3. Analysis of the signal power spectrum

To define the form of the power spectrum of the signal $u_s(t)$, we assume a definition of the power spectrum which is quite often used in technology:

$$S(\omega) = \lim_{T\to\infty} \frac{1}{2T} \left| \int_{-T}^{T} u_s(t) \exp(-j\omega t)\, dt \right|^2, \tag{13}$$

where $u_s(t)$ is the time form of the signal and $S(\omega)$ is the power spectrum of the signal.

For the signal $u_s(t)$ (formula (12)) $S(\omega)$ is expressed as

$$S(\omega) = \lim_{T\to\infty} \frac{1}{2T} \left| \int_{-T}^{T} \text{const} \left[\sum_{n=-\infty}^{+\infty} \delta(t - n\tau_p - t_r) \right] \left[\sum_{i=1}^{N} a_i H(\boldsymbol{r}_i) \times \right. \right.$$

$$\left. \left. \times \cos(\omega_i t + a_i + \gamma_i) \exp(-j\omega t)\, dt \right| ^2 . \right. \tag{14}$$

The first term (under the integral) of the signal, which contains the sum of the Dirac impulses, corresponds to the signal sampling. In the spectral representation, it involves the existence of successive copies of the spectrum of the second term, which are distant by

$$\omega_p = 2\pi \frac{1}{\tau_p}. \tag{15}$$

By assuming that the spectrum of the second term describing the signal is limited and zero for $\omega > \omega_p/2$, we only consider the spectrum concentrated round the pulsation equal to zero. It corresponds to the practical signal filtration narrowing its band to the useful interval $(0; \omega_p/2)$. Thus, we obtain

$$S(\omega) = \lim_{T\to\infty} \frac{1}{2T} \left| \int_{-T}^{T} \text{const} \left[\sum_{i=1}^{N} a_i H(\boldsymbol{r}_i) \cos(\omega_i t + a_i + \gamma_i) \times \right. \right.$$

$$\left. \left. \times \exp(-j\omega t)\, dt \right| ^2 . \right. \tag{16}$$

Let us denote the terms which we achieve as the integral has been introduced under the sum sign as

$$F_i(j\omega) = \left| \int_{-T}^{T} a_i H(\boldsymbol{r}_i) \cos(\omega_i t + a_i + \gamma_i) \exp(-j\omega t)\, dt \right|^2. \tag{17}$$

By substituting this determination in formula (16) and calculating the squared modulus of the sum, we obtain

$$S(\omega) = \text{const} \lim_{T\to\infty} \frac{1}{2T}\left[\sum_{i=1}^{N} R_2^2 F_i(j\omega) + \sum_{i=1}^{N} \operatorname{Im}^2 F_i(j\omega)\right] +$$

$$+ \lim_{T\to\infty} \frac{1}{2T}\left(\sum_{k=1}^{N}\sum_{i=1}^{N} [\operatorname{Re} F_k(j\omega) \operatorname{Re} F_i(j\omega) + \operatorname{Im} F_k(j\omega) \operatorname{Im} F_i(j\omega)]\right). \quad (18)$$

The second term in formula (18) applies to the products of functions of independent scatterings and is zero.

Thus, the signal spectrum becomes

$$S(\omega) = \text{const} \lim_{T\to\infty} \frac{1}{2T} \sum_{i=1}^{N} a_i^2 \left| \int_{-T}^{T} H(\boldsymbol{r}_i) \cos(\omega_i t + a_i + \gamma_i) \exp(-j\omega t)\, dt \right|^2. \quad (19)$$

For our signal the operation of passing to the limit in time causes the fact that the number of particles giving the spectral components should tend to infinity. And the integrals in formula (19) will tend to the Fourier transforms of the subintegral functions. These transforms exist, as the subintegral functions are limited in time in view of the bounded dimensions of the sample volume. Thus, the components of the sum can be replaced by the squared moduli of the respective Fourier transforms. We denote as $\mathscr{F}$ the Fourier transformation. By calculating the squared modulus of the Fourier transform of the subintegral function, on the assumption that $\mathscr{F}[H(\boldsymbol{r}_i) = 0]$ for $|\omega| > \omega_i$ we obtain the dependence

$$|\mathscr{F}[H(\boldsymbol{r}_i)\cos(\omega_i t + a_i + \gamma_i)]|^2$$
$$= |\mathscr{F}[H(\boldsymbol{r}_i)]|^2 * \delta(\omega + \omega_i) + |\mathscr{F}[H(\boldsymbol{r}_i)]|^2 * \delta(\omega - \omega_i). \quad (20)$$

The sum from formula (18) should be extended to all particles flowing through the sample volume in the measurement time. We shall denote it as a boundary transition, by designating as M the number of particles which are summed up. We replace the normalising factor $1/T$ by $1/M$. Since the random variable a_i is, when squared, averaged, and its mean square value $\overline{(a^2)}$ can be made part of the constant term, we obtain

$$S(\omega) = \text{const} \lim_{M\to\infty} \frac{1}{M} \sum_{i=1}^{M} \left(|\mathscr{F}[H(\boldsymbol{r}_i)]|^2 * \delta(\omega + \omega_i) + |\mathscr{F}[H(\boldsymbol{r}_i)]|^2 * \delta(\omega - \omega_i)\right), \quad (21)$$

or otherwise

$$S(\omega) = \text{const}\left(\lim_{M\to\infty} \frac{1}{M} \sum_{i=1}^{M} |\mathscr{F}[H(\boldsymbol{r}_i)]|^2 * \delta(\omega + \omega_i) + \right.$$
$$\left. + \lim_{M\to\infty} \frac{1}{M} \sum_{i=1}^{M} |\mathscr{F}[H(r_i)]|^2 * \delta(\omega - \omega_i)\right). \quad (22)$$

The signal power spectrum, expressed by formula (22), consists of two identical and separate, in view of the assumption $\mathscr{F}[H(\boldsymbol{r}_i)] = 0$ for $|\omega| > \omega_i$, components situated on the pulsation axis symmetrically with respect to zero.

In the further part, considerations will be limited to one of those components only, ie., the one on the positive semi-axis of pulsation, so as to shorten the notation of the formula. In addition, we shall neglect the constant proportionality factor. Thus, we obtain the simple form of the spectrum:

$$S(\omega) = \lim_{M\to\infty} \frac{1}{M} \sum_{i=1}^{M} |\mathscr{F}[H(\boldsymbol{r}_i)]|^2 * \delta(\omega - \omega_i). \tag{23}$$

The next transformation executed here is now strictly related to the numerical nature of the description of the spectrum to be constructed. The continuous velocity axis will be replaced by a discrete one. I.e., we assume that the velocity, and, thus, the Doppler frequency, will take a finite number of values, whereas the two adjacent quantities differ by a finite quantity, called the discretization step.

This way of frequency representation permits the next spectrum transformation to be carried out. Among the components of the sum represented in formula (23), let us choose those in which the Doppler frequency ω_k is the same. They are the components of the spectrum from particles moving at the same velocity. First, the separability of the convolution operation with respect to addition permits us to sum up the contributions from these factors, and then convolute the result with the Dirac delta, corresponding to this frequency. For the velocity v_k the summation result will be:

$$\delta(\omega - \omega_k) * \left(\lim_{M_k\to\infty} \frac{1}{M_k} \sum_{i=1}^{M_k} |\mathscr{F}[H(\boldsymbol{r}_i)]|^2 \right). \tag{24}$$

To get the whole spectrum, the above contributions must be summed up for all velocities:

$$S(\omega) = \sum_{k=1}^{L} \left\{ \delta(\omega - \omega_k) * \left(\lim_{M_k\to\infty} \frac{1}{M_k} \sum_{i=1}^{M_k} |\mathscr{F}[H(\boldsymbol{r}_i)]|^2 \right) \right\}, \tag{25}$$

where L is the number of discrete values of velocity in the vessel.

In the spectral form, the internal sum according to the index i represents the effect of a passage through the sample volume of particles at velocity corresponding to the frequency ω_k. Indeed, a time change in $\boldsymbol{r}_i$ corresponds to the particle path through the sample volume, while $H(\boldsymbol{r}_i)$ describes a change in the scattered acoustic energy in passing through the sample volume. The external sum, according to the index k corresponds to the summation of the effects for all the particle motion velocities existing in the sample volume.

We can note that the existence of a large number of velocities in the sample volume can result from the presence of a specific velocity profile in the vessel.

It can also result from instantaneous velocity oscillations related to the flow perturbations. Since the estimation of the signal spectrum directly from its temporary form, as used here and applied generally in analysing equipment, requires a very long observation time, it is not possible to distinguish between the contributions from the velocity gradient and the instantaneous oscillations. In other words, having only the signal spectrum, we cannot say whether there are instantaneous velocity perturbations, since the effect of a constant velocity gradient on the spectrum can be the same. To be able to make this distinction, we must have more information on the flow. Let us assume that we know the mean velocity profile in the sample volume, for such a profile can be measured by a pulsed flowmeter in the same time in which we collect data for spectral analysis. Knowing the flow profile in the vessel the position and shape of the measurement volume, we can, e.g. by numerical calculations, try to find the spectrum $S(\omega)$ of the signal, by calculating successively the functions $H(\boldsymbol{r}_i)$ and their Fourier transforms. In practice, it is, however, very difficult, mainly because of the geometrical complexity of the function $H(\boldsymbol{r}_i)$. Let us then use approximations. First, we shall calculate the energy distribution of scattered waves as a function of velocity. In other words, for each frequency ω_k, some distribution of the power of the scattered wave $B_k(\omega)$

$$B_k(\omega) = \lim_{M_k \to \infty} \frac{1}{M_k} \sum_{i=1}^{M_k} |\mathscr{F}[H(\boldsymbol{r}_i)]|^2, \tag{26}$$

caused by the effect of particles passing through the sample volume, will be replaced by a line of the same power from the appropriate distribution.

$$P_k = \int_{-\infty}^{+\infty} B_k(\omega)\, d\omega. \tag{27}$$

Thus, the power distribution of scattered waves as a function of velocity is given by the formula

$$S_G(\omega) = \sum_{k=1}^{L} P_k \delta(\omega - \omega_k), \tag{28}$$

for each of the frequencies ω_k is, from the Doppler formula, related to the the respective velocity v_k.

Let us note that distribution (28) would correspond to the spectrum of the Doppler signal if we neglected the effect of the finite time of the particle passage through the sample volume. For if $H(\boldsymbol{r}_i)$ were functions changing very slowly in time, their spectra would be very strongly concentrated close to zero, i.e., equal practically to the constants P_k introduced here. This would require that the width of the spectrum of the function $H(\boldsymbol{r}_i)$ should be negligible with respect to the quantities ω_k.

4. Numerical model synthesis

The spectrum analysis is now at a moment where as a result of the simplifications used, it is easy to introduce numerical calculations, to calculate for known parameters the specific form of the power distribution of the received signal as a function of velocity (formula (28)).

It is easier to calculate this distribution in a way other than that resulting from the analysis carried out. Instead of following the paths of particular particles, we should calculate the sums of the powers existing at these points of the sample volume where the velocity is constant [14]. Since we cannot neglect the effect of the finite time of the particle passage through the sample volume, for it influences greatly the spectral shape, some approximation was added to the numerical calculations. To some limited extent, the flow perturbations will also be considered in the model built. Its construction will begin with representing an approximation of the particle passage effect (the transit time effect).

For each discrete value of the velocity v_k related to ω_k, we introduce an arbitrary approximation of this effect, as

$$B_k(\omega) = P_k N(0, \sigma_k), \tag{29}$$

where

$$N(0, \sigma_k) = \frac{1}{\sqrt{\sigma_k}} \exp(-\omega^2/2\sigma_k^2). \tag{30}$$

$N(0, \sigma_k)$ is thus a Gaussian function symmetrical with respect to zero, with a standard deviation σ_k.

For each velocity v_k the shape of the fuzziness of the power spectrum was approximated by a Gaussian curve. The coefficient P_k ensures equality of the total scattered power for each velocity v_k between our approximation and the exact value. We shall define intuitively the width of the Gaussian curve as an approximation of the transit time effect, expressed by σ_k, and then the value of the whole approximation will be verified experimentally.

It follows from considerations made in the conclusion of the previous section that for a given sample volume the width of fuzziness of the power spectrum is the greater the shorter the time spent by particles in the sample volume. Thus, this width should be proportional to the particle velocity and inversely proportional to the length of the particle path in the sample volume. The particle velocity is a known parameter. Unfortunately, it is difficult to determine the length of the particle path in the sample volume. However, it should be expected that the power P_k scattered by particles moving at the velocity v_k is related to the mean particle path length at this velocity in the sample volume. The deviation σ_k can thus be defined in the following way:

$$\sigma_k = \frac{v_k}{b(P_k)^{1/\beta}}, \tag{31}$$

where b and β are constant parameters determined experimentally from the dependence on the geometry of the sample volume. The above approximation resembles the one which Gabrini used successfully in [6].

For the purposes of our model of the Doppler signal spectrum, it is convenient to desscribe perturbed flow through the mean profile of this flow and instantaneous velocity fluctuations round this profile, Anyway, this description is accepted in fluid mechanics [17]. Let $\bar{v}_k$ denote the mean velocity in the elementary volume ΔV_i, resulting from the position of the sample volume with respect to the mean velocity profile in the vessel. We denote as $p_i(v)$ the probability that the instantaneous velocity $\mathrm{v} = \bar{v}_k + v$ occurs at this point. Thus, v denotes the difference between the instantaneous and mean velocities. We continue to maintain the assumption that the velocity is parallel to the axis of the vessel. For strongly perturbed flows, in stenotic vessels, and for pulsating flows, unfortunately, this assumption can deviate strongly from reality. When the measurement time is sufficiently long, the power scattered in the elementary fragment of the sample volume ΔV_i (Fig. 2), defined as $dH^2(\xi_i)$,

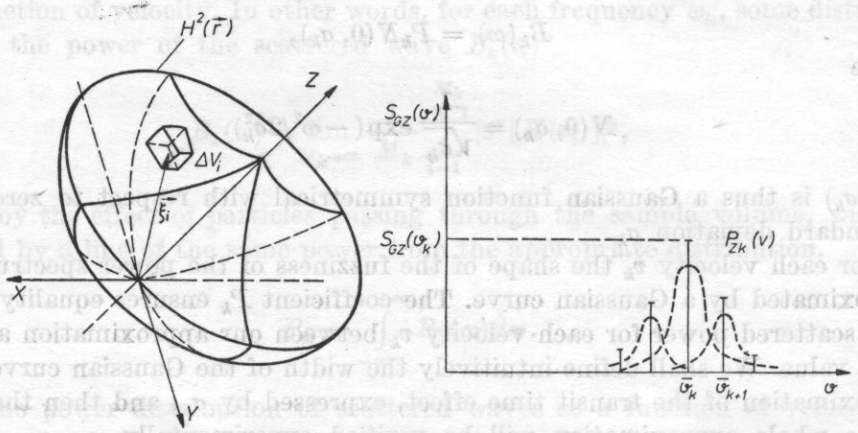

Fig. 2. The idea of the numerical calculations of the power spectrum of scattered waves as a function of velocity ΔV_i — the elementary fragment of the sample volume, $H^2(\boldsymbol{r})$ — the sample volume, $P_{zk}(v)$ — the probability distribution of the deviation of the instantaneous velocity by v from the mean velocity $\bar{v}_k$

is divided among all the velocities occurring in ΔV_i, in proportion to their occurrence frequency, defined by $p_i(v)$. The vector ξ_i denotes the position of each of the elementary fragments of the sample volume ΔV_i (Fig. 2). By summing up all the powers related to the given mean velocity $\bar{v}_k$, we obtain the magnitude of power related to this velocity:

$$P_{zk}(v) = \sum_{i=1}^{I_k} \Delta V_i dH^2(\xi_i) p_i(v). \tag{32}$$

Instead of the line of the power P_k, just as in the case of laminar flow, we obtain a certain distribution on the velocity axis. When $p_i(v)$ is constant, we obtain, in all the elementary volumes, where v_k is the same:

$$P_{zk}(v) = p_k(v) \sum_{i=1}^{I_k} \Delta V_i dH^2(\xi_i), \tag{33}$$

where $p_k(v)$ is the probability that v deviates from the mean velocity at those points where it equals $\bar{v}_k$. Thus, this probability is now related to the velocity profile and not to the space.

The latter formula can be changed to the form

$$P_{zk}(v) = p_k(v) P_k. \tag{34}$$

The values of P_k are defined by the sum in formula (33) and refer to the mean velocity profile. Thus, the power distribution of the Doppler signal as a function of velocity becomes

$$S_{Gz}(v) = \sum_{k=1}^{L} P_k p_k(v) * \delta(v - v_k). \tag{35}$$

This distribution contains two factors with a significant effect on the width and shape of the signal power spectrum. They are the flow perturbations and the existence of the mean velocity gradient in the measurement volume. It should be completed by the effect of the finite time of the particle passage. When the flow perturbations are not too large, we can approximate this effect, just as for laminar flow, from the mean velocity profile. Thus, just as we did previously, for each discrete value of the mean velocity $\bar{v}_k$ we introduce the Gaussian curve $N(0, \sigma_k)$ as its approximation. The standard deviation σ_k is defined as previously from formula (31), thus, it is based on the values of P_k defined by the mean flow profile. However, because of the existence of flow perturbations, the transit time effect will be divided among all the instantaneous velocities occurring round the mean $\bar{v}_k$ in proportion to their occurrence frequency, i.e., $p_k(v)$. This division of the transit time effect between the velocity distribution is expressed by a convolution of the functions $p_k(v)$ and $N(0, \sigma_k)$ for each mean velocity $\bar{v}_k$.

By transforming the velocity axis into the frequency one according to the Doppler formula, we obtain a complete approximation of the spectrum as

$$S_s(\omega) = \sum_{k=1}^{L} \left[P_k N(\omega_k, \sigma_k) * p_k(\omega) \right]. \tag{36}$$

Equation (36) is the final form of our model of the power spectrum of the Doppler signal.

5. Mean value and the standard deviation of frequency in the power spectrum

From the final form of the spectrum approximation, we can calculate its mean value and the standard deviation, in order to investigate the relationships between these quantities and the flow parameters.

We obtain, as the mean frequency in the spectrum,

$$\overline{\omega}_s = \frac{\int\limits_{-\infty}^{+\infty} \omega S_s(\omega)\, d\omega}{\int\limits_{-\infty}^{+\infty} S_s(\omega)\, d\omega} = \frac{\sum\limits_{k=1}^{L} P_k \omega_k}{\sum\limits_{k=1}^{L} P_k}. \tag{37}$$

In view of the direct relationship between ω_k and v_k, the mean frequency in the spectrum corresponds to the mean bulk velocity weighted in the sample volume. The weights P_k are defined by the power distribution in the sample volume and its position with respect to the flow profile. We can note that the mean frequency does not depend on the transit time effect or the possible perturbations. This results from our assumptions as to the effects mentioned above. In practice, some nonsymmetricities can certainly occur, as a result of the out-of-parrallel character of the velocity vectors with respect to the vessel axis and the nonsymmetricity of the transit effect $B_k(\omega)$, described by equation (26).

It is much more interesting to consider the result of the calculations of the standard deviation of the power spectrum. By calculating the variance of the spectrum $S_s(\omega)$, we obtain

$$\sigma_s^2 = \frac{\sum\limits_{k=1}^{L} P_k \omega_k^2}{\sum\limits_{k=1}^{L} P_k} - \overline{\omega}_s^2 + \frac{\sum\limits_{k=1}^{L} P_k \sigma_k^2}{\sum\limits_{k=1}^{L} P_k} + \frac{\sum\limits_{k=1}^{L} P_k \sigma_{pk}^2}{\sum\limits_{k=1}^{L} P_k}, \tag{38}$$

where σ_{pk}^2 is the variance of the distribution $p_k(\omega)$.

The expression describing the variance σ_S^2 of our approximation of the spectrum contains three distinguishable components. The first is the effect of the mean velocity gradient. We denote it as

$$\sigma_G^2 = \frac{\sum\limits_{k=1}^{L} P_k \omega_k^2}{\sum\limits_{k=1}^{L} P_k} - \overline{\omega}_s^2. \tag{39}$$

The variance σ_G^2 defines the spectrum width when the effect of the transit time and the flow perturbation are negligible. Another one, denoted by σ_T^2, is related

to the effect of the finite time of the particle passage through the sample volume:

$$\sigma_T^2 = \frac{\sum_{k=1}^{L} P_k \sigma_k^2}{\sum_{k=1}^{L} P_k}. \tag{40}$$

A third component in turn is related to the flow perturbations:

$$\sigma_Z^2 = \frac{\sum_{k=1}^{L} P_k \sigma_{pk}^2}{\sum_{k=1}^{L} P_k}. \tag{41}$$

Both σ_T^2 and σ_Z^2 are certain mean values of the influence of the effects of the transit time and flow perturbations, related to the power distribution in the sample volume and its position with respect to the mean profile of flow through the values of P_k.

By using the new notation, we can write the total variance of the spectrum as

$$\sigma_S^2 = \sigma_G^2 + \sigma_T^2 + \sigma_Z^2. \tag{42}$$

The numerical model presented here permits the calculation of the shape and parameters of the power spectrum and the separation of the contributions from the different factors to the spectrum, and, by it, also, an accurate measurement of the flow parameters, namely σ_{pk}^2. For we can, by identifying σ_S^2 through measurements, calculate the values of σ_G^2 and σ_T^2, and then calculate the value of σ_Z^2. When we assume that σ_{pk} is constant throughout the sample volume, σ_{pk} is equal to σ_Z.

6. Experimental studies on the model of the power spectrum of the Doppler signal

By using the numerical synthesis of the power spectrum of the Doppler signal given above, we calculated the spectra of a signal for laminar flows. The results obtained were compared with the measured results. Thus, we verified the calculations of the effect of the velocity gradient in the sample volume and the effect of the transit time on the shape and parameters of the spectrum.

Looking at the results we can say that the elaborated description of the Doppler signal corresponds well to reality. We observed, however, a certain difference between the mean frequencies of the measured and calculated spectra, which is absent from Figs. 3 and 4, for it was compensated for in the course of matching the peaks of respective curves. The existence of this difference can be explained by an inacuracy of the model and also by the differences

between the real and calculated positions of the sample volume, or by slow changes in the output of the pump in the course of recording signals. These differences were compensated for numerically by a change in the value of the maximum velocity used as the calculation parameter. We should point out that these differences were always smaller than 2.5% of the maximum velocity; thus, quite low.

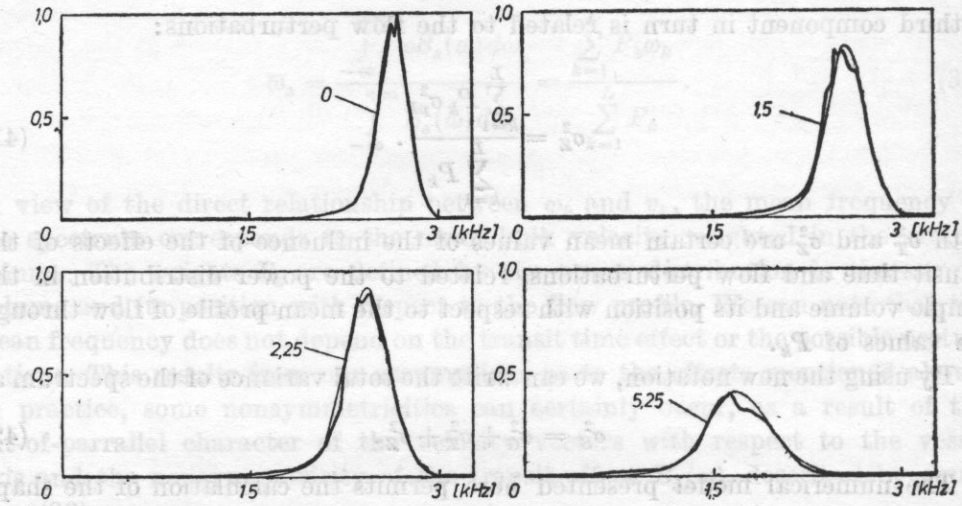

Fig. 3. The measured and calculated power spectra of the Doppler signal for flow with the Reynolds number $Re = 1450$. Thick line — measurements, thin line — calculations

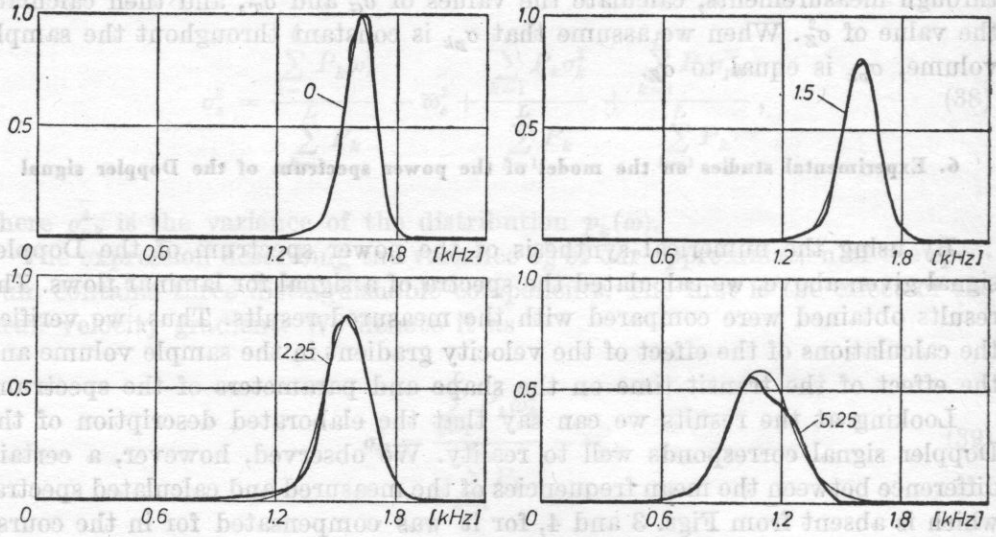

Fig. 4. The measured and calculated power spectra of the signal for flow with the Reynolds number $Re = 700$. Thick line — measurements, thin line —calculations

The parameters of the spectra shown in Figs. 3 and 4 are given in Table 1. It contains the mean values and the standard deviations of the measured spectra f_m and σ_m and the calculated ones, f_s and σ_s, and also the values of the relative errors between these quantities.

Table 1

Re	Sample volume position	f_m [Hz]	f_s [Hz]	[%]	σ_m [Hz]	σ_s [Hz]	[%]
1450	0	2619.30	2623.29	0.20	119.34	118.70	0.50
	1.5	2542.61	2536.71	0.17	159.89	148.98	6.82
	2.25	2543.70	2428.20	0.14	179.58	176.59	1.56
	5.25	1656.30	1666.80	0.63	231.64	232.55	0.39
700	0	1677.40	1616.50	0.17	77.01	173.31	4.80
	1.5	1610.20	1608.30	0.14	94.41	94.44	0.30
	2.25	1571.50	1571.40	0.01	114.28	113.53	0.66
	5.25	1091.90	1092.97	0.10	146.41	152.49	4.15

The differences between the parameters of the measurement curves and the results of a numerical synthesis of the spectrum, contained in Table 1, are random in nature. They suggest, however, the necessity for a more precise implementation of measurements. In the present case, the pipe wall caused a deformation in the sample volume with respect to the assumed symmetry. This explains perhaps the irregular shape of the spectra for the position "5.25" of the sample volume.

The experimental studies on the correctness of the model, though still distinctly incomplete, confirmed the usefulness of the approximation of the finite transite time effect. These studies confirm that the present model traces well the relative changes in the contribution in the spectrum width of the mean velocity gradient and the effect of the transit time.

7. Turbulence index

The achieved relationships between the parameters of the spectrum and the flow, (37) and (38), indicate that the initially discussed perturbation index, defined by the parameters of the spectrum, can significantly deviate from values characterizing the velocity distribution.

We now present the results of the application of the classical perturbation index and those obtained when using the corrected turbulence index in the case of the application of these indices for turbulent flow with a Reynolds number of 5000. As was mentioned above, equation (42) can serve in determining the effect of the flow parameters on the power spectrum. By transforming this

equation slightly, we obtain

$$\sigma_Z^2 = \sigma_S^2 - \sigma_T^2 - \sigma_G^2. \tag{43}$$

If we assume that the presented results of the verification of the model prove its correctness, the value of the calculated variance σ_S^2 is equal to the variance σ_m^2 which was measured. The sum of the variance σ_T^2 and σ_G^2 is the variance of the power spectrum for laminar flow with the same profile as the mean one of the perturbed flow under study. The value of this sum, denoted by σ_{SL}^2, can be calculated by means of our model. Thus, we obtain the following expression of the averaged flow perturbations, determined from formula (41),

$$\sigma_Z = \sqrt{\sigma_m^2 - \sigma_{SL}^2} \tag{44}$$

In other words, the expansion of the spectrum, caused by flow perturbations, equals a square root from the difference between the measured and calculated spectrum variances for the mean profile of perturbed flow.

Table 2 shows the values of the perturbation index, defined classically as σ_m/f_m, the index calculated from numerical results of σ_s/f_s and the values of the corrected perturbation index σ_Z/f_m.

Table 2

Re	Sample volume position	σ_m/f_m [%]	σ_{SL}/f_{SL} [%]	σ_Z/f_m [%]	$\frac{\sigma_Z}{f_m}\frac{\Delta\sigma_Z}{\sigma_Z}$ [%]
1450	0	4.56	4.52	0.47	±4.34
	1.5	6.29	5.87	2.28	±1.50
	2.25	7.38	7.27	1.30	±1.26
	5.25	13.99	13.95	1.24	±15.88
700	0	4.76	4.52	1.46	±1.42
	1.5	5.86	5.87	0.15	±23.61
	2.25	7.22	7.27	0.83	±6.26
	5.25	13.47	13.95	3.90	±4.99
5000	0	12.06	2.66	11.76	±0.59

It follows from the data given in Table 2 that for laminar flows under study, the values of the corrected perturbation index are, however, different from zero. It means a lack of correctness in evaluating the flow perturbations by means of this method. By analyzing the effect of error on the evaluation of perturbations, we can explain these inaccuracies.

From equation (44), we can determine the effect of the error involved in the calculations of the spectrum variance, on the effect of the error characteristic of the calculated flow perturbations:

$$\frac{\Delta\sigma_Z}{\sigma_Z} = \frac{1}{1-\sigma_m^2/\sigma_{SL}^2}\frac{\Delta\sigma_{SL}}{\sigma_{SL}}, \tag{45}$$

where $\Delta\sigma_Z/\sigma_Z$ is the relative error in evaluating the value of perturbations; $\Delta\sigma_{SL}/\sigma_{SL}$ is the relative calculation error.

Fig. 5 represents two curves illustrating this dependence on two different values of the ratio σ_m/σ_{SL}. For $\sigma_{SL} \ll \sigma_m$, the effect of the velocity gradient and the transit time effect on the spectrum variance is small compared with

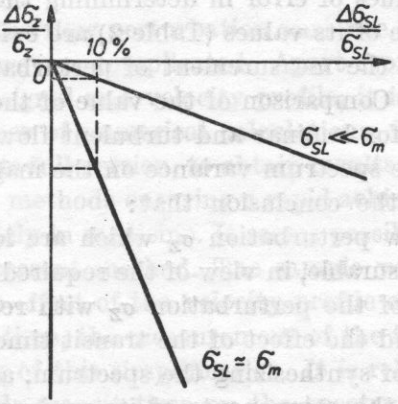

Fig. 5. The relative error of the calculation of the flow perturbation variance $\Delta\sigma_Z/\sigma_Z$ as a function of the relative error of numerical calculations $\Delta\sigma_{SL}/\sigma_{SL}$

the effect of perturbations. In this case, the calculation inaccuracy is hardly significant for the exactness of the perturbation determination. Unfortunately, in the opposite case, if perturbations are small compared with the other effects expanding the spectrum, $\sigma_m \simeq \sigma_{SL}$. Then, even small error in the calculation σ_{SL} causes error of as much as dozens of % in estimating the perturbation degree. In this case, the achieved magnitude of the corrected perturbation index can involve such significant error that it cannot be interpreted as a result of real flow perturbations.

On the basis of the relative differences between the values of σ_m and σ_S, in Table 1, we are justified in stating that the accuracy of the calculations of $\Delta\sigma_{SL}/\sigma_{SL}$ is better than 10%. With this assumption, error in estimating the magnitude of the corrected perturbation index was calculated from formula (44). The absolute value of this error was set in the last column of Table 2.

8. Discussion and conclusions

The conclusions from the application of the corrected perturbation index for the flows under study are as follows:

1. In keeping with the predictions from Section 3, the effect of the mean velocity gradient and that of the transit time on the spectrum is similar to the

effect of perturbations. Thus, the perturbation index is not unambiguously related to the flow perturbations. Its values obtained for the position "5.25" of the sample volume and laminar flow are greater than those for turbulent flow.

2. The corrected perturbation index determines much better the real perturbations in flow. However, it is much more complicated to calculate its value, requiring knowledge of the flow parameter, which the mean profile is.

3. The enormous values of error in determining the corrected perturbation index, obtained for some of its values (Table 2) are evidence of the low sensitivity of the method for the measurement of perturbations through spectrum variance measurements. Comparison of the value of the corrected perturbation index and its accuracy for laminar and turbulent flows, and also the analysis of the dependence of the spectrum variance on the magnitude of perturbations (formula (45)) lead to the conclusion that:

— values of the flow perturbation σ_Z which are low with respect to σ_{SL}, are particularly not measurable, in view of the required measurement accuracy;

— for large values of the perturbation σ_Z with respect to σ_{SL}, the effect of the mean gradient and the effect of the transit time are actually negligible.

The numerical way of synthesizing the spectrum, as presented here, makes it possible to calculate the components of its variance, corresponding to the contributions from the mean velocity gradient and the transit time effect. This permits the calculation of the mean variance of perturbations in the sample volume, from relation (42). It is also the basis for the evaluation and interpretation of the results of perturbation measurements, and also of the optimization of the parameters of equipment, depending on the measured flow parameters.

However, relation (38) is concerned with the variance of full spectrum distributions. In practice, we are forced, as a result of the occurrence of equipment noise, to fix the lower level to which the measured results are considered significant. This can introduce inaccurracies in using this relation, since, usually, the sum of the variances of cut-off distributions is different from the variance of the cut-off resultant distribution.

In the extreme cases, the present model reduces, for the laminar flow, to the forms described in the literature:

— when the transit time effect is negligible, the spectrum obtained from calculations corresponds to the velocity distribution in the sample volume [15];

— when the mean velocity gradient in the sample volume is negligible, the spectrum has the shape of a Gaussian function with its width proportional to the velocity. It corresponds to the results achived by GABRINI [6].

For perturbed flow, when the mean velocity gradient and the transit time effect are negligible, the shape of the spectrum corresponds to the occurrence frequency of the instantaneous velocity averaged over the sample volume. We can calculate the mean perturbation variance from in vivo measurements. The necessary data include:

a. the mean flow profile, which can be determined e.g. by a multi-gate pulsed flowmeter;

b. the position of the sample volume, which can be determined e.g. by selecting for the multi-gate analysis a signal from one gate of the profile-measuring equipment;

c. the shape of the sample volume which we can determine irrespective of the flow under study.

The calculations of the flow perturbation variance, as presented in the previous sections, are, however, complicated. Apart from measurements of the power spectrum of the signal and velocity profile, it is necessary each time to carry out a large number of numerical calculations. This prevents the use of the present method, in its full version, to obtain results in real time. It is a serious difficulty, since only methods ensuring a rapid achievement of results can be expected to be used widely in medicine. It seems possible, in turn, to use a simplified version of the present method. The sample volume applied should be so small as to make the effect of the velocity profile on the spectrum variance negligible. At the same time, the measurement of the flow profile would ensure control of permissibility of this simplification. It is relatively easy to calculate the effect of the particle transit time on the spectrum variance in this case. By identifying this effect and detracting it from the spectrum, we obtain quite an accurate value of the mean variance of the flow perturbations.

Acknowledgement. The author wishes to thank Prof. L. FILIPCZYŃSKI for discussion and a number of valuable remarks in the course of preparing this paper.

References

[1] B. A. J. ANGELSEN, *A theoretical study of scattering of ultrasound from blood*, IEEE Trans. Biom. Enging., **27**, 2 (1980).

[2] W. R. BRODY, I. D. MEINDL, *Theoretical analysis of the C. W. Doppler ultrasonic flowmeter*, IEEE Trans. Biom. Enging., **21**, 3, 183–192 (1974).

[3] L. FILIPCZYŃSKI, R. HERCZYŃSKI, A. NOWICKI, T. POWAŁOWSKI, *Blood flows — hemodynamics and ultrasonic Doppler measurement methods* (in Polish), PWN, 1980.

[4] L. FILIPCZYŃSKI, *Detectability of gas bubbles in blood by the ultrasonic method* (in Polish), Archiwum Akustyki, **18**, 1, 11–30 (1983).

[5] F. K. FORSTER, *The applications and limitations of Doppler spectral broadening measurements for the detection of cardiovascular disorders*, Ultrasound in Med. Biol., D. White, R. Brown (eds.), Plenum Press, **3B**, 1223–1226 (1977).

[6] J. L. GABRINI, F. K. FORSTER, J. E. JORGENSEN, *Measurement of fluid turbulence based on pulsed ultrasound techniques*, Part 1 and Part 2, J. Fluid Mech., **118**, 445–470, 471–505 (1982).

[7] J. E. JORGENSEN, D. N. CAMPAU, D. W. BAKER, *Physical characteristics and mathematical modelling of pulsed ultrasonic flowmeter*, Med. Biol. Enging., **12**, 4, 404–420 (1973).

[8] J. P. MOUTET, *Etudes des modifications de l'ecculment induites par une stenose arterielle, these de doctorat,* es — sciences naturelles, Paris, 1981.

[9] V. L. NEWHOUSE, P. J. BENDICK, L. W. VARNER, *Analysis of transit time effects on Doppler flow measurement, IEEE,* Trans. Biom. Enging., **23**, 5 (1976).

[10] A. NOWICKI, *Ultrasonic Doppler pulsed method and equipment for blood flow measurements in the circulation system* (in Polish), D. Sc. Thesis, IPPT PAN, Warsaw, 1975.

[11] A. V. OPPENHEIM, R. W. SCHAFER, *Digital signal processing,* Prentice Hall, Inc., Englewood Cliffs, New Jersey, 1975.

[12] A. PAPOULIS, *Probability, random variables and stochastic processes* (in Polish), WNT, Warsaw, 1972.

[13] P. PERRONNEAU, M. PIECHOCKI, J. P. MOUTET, *Contribution des conditions de mesure et des caracteristiques de l'ecoulement sanguin a la genese des spectres Doppler,* Colloque sur les Ultrasons et l'acoustique phisique, Paris, November 1982.

[14] M. PIECHOCKI, *Ultrasonic Doppler methods of measurements of perturbed blood flows* (in Polish), D.Sc. Thesis, IPPT PAN, 1983.

[15] T. POWAŁOWSKI, *Mesaurement of fluid flow by the ultrasonic Doppler C.W. method* (in Polish), D. Sc. Thesis, IPPT PAN, Warsaw, 1976.

[16] K. K. SHUNG, R. A. SINGLEMANN, J. M. REID, *Scattering of ultrasound by blood,* IEEE, Trans. Biomed. Enging., **23**, 6, 460–467 (1976).

[17] E. TULISZKA, *Fluid mechanics* (in Polish), PWN, Warsaw, 1980.

[18] J. WESŁOWSKI, *Experimental and clinical studies on the usefulnees of ultrasound in vascular surgery* (in Polish), Ass. Prof. Thesis, Reports IPPT PAN, Warsaw, 1982.